

# Jets and the Accretion Flow in Low Luminosity Black Holes

Emma Gardner and Chris Done

Submitted to MNRAS

## ABSTRACT

We present a broadband (radio - X-rays) spectral model for black hole binaries (BHBs) in the low/hard state (LHS). We model the accretion flow as a disc which is replaced in the inner regions by a radiatively inefficient hot flow. The flow emits cyclo-synchrotron radiation, which produces another source of seed photons for Compton scattering as well as those intercepted from the outer disc. We balance heating with Compton cooling to derive the electron temperature self-consistently, and find the dominant source of seed photons changes from disc to cyclo-synchrotron emission as accretion rate drops and the disc recedes. This reproduces the observed behaviour of the X-ray spectral index, which initially hardens with decreasing accretion rate, and then softens again.

We include a conical synchrotron jet of constant bulk Lorentz factor with parameters based on those observed from a bright low/hard state in GX339-4. This model reproduces the observed  $L_R \propto L_X^{0.7}$  radio-X-ray correlation as expected for a jet where the magnetic energy density and particle density scale with  $\propto \dot{m}$ . The kinetic energy of the jet also scales as  $\propto \dot{m}$ , but its optically thin synchrotron luminosity scales as  $\propto \dot{m}^2$  as it is determined by the product of the electron and magnetic energy densities. Thus the X-rays from the jet are as radiatively inefficient as the X-rays from the hot flow and there is no transition from an accretion flow dominated state to a jet dominated state in the X-ray emission in these models.

**Key words:** X-rays: accretion discs, black hole physics

## 1 INTRODUCTION

The low/hard state (LHS) of black hole binaries (BHB) is typically seen at mass accretion rates below a few per cent of the Eddington limit. It is characterized by a hard X-ray spectrum, rising in  $\nu f_\nu$  to a peak at a few hundred keV, in sharp contrast to the typical temperature of a few hundred eV expected from an optically thick, geometrically thin accretion disc. These X-rays are also strongly variable on short (sub second) timescales, again, in sharp contrast to the long (few hour) viscous timescale expected from even the innermost radii of a thin disc. These properties instead are more typical of the alternative set of solutions of the accretion flow equations, where the flow is geometrically thick, and optically thin. The most well known of these alternative solutions are the Advection Dominated Accretion Flow (ADAF) models (Narayan & Yi 1995), but these are only an analytic approximation to what is almost certainly a more complex solution, as the flow must be threaded by magnetic fields. Differential rotation shears the field azimuthally, while buoyancy lifts it vertically, and the combination sets up a turbulent magnetic dynamo which acts to transport angular momentum outwards so material can fall inwards. Close to the horizon, this turbulent field can also produce a jet, as observed in this state (see e.g. the review by Done, Gierlinski & Kubota 2007 hereafter DGK07)

These hot flow solutions are only possible at low mass accretion rates, collapsing to the standard disc solutions when the flow becomes optically thick. This gives a mechanism for the dramatic

hard to soft state transition seen in the BHB, and the associated collapse of the radio jet. This transition is complex, but the data can be largely fit into a picture where the thin disc progressively replaces the hot flow down to smaller radii as the mass accretion rate increases. These truncated disc models predict that the contribution from the thin disc becomes stronger with increasing mass accretion rate, increasing the seed photons for Compton cooling of the hot flow, so the hard X-ray spectrum becomes softer, as observed. All timescales associated with the disc truncation radius will decrease, giving a qualitative (and now quantitative) framework in which to explain the correlated increase in characteristic frequencies of the time variability (DGK07, Ingram, Done & Fragile 2009; Ingram & Done 2011; 2012).

While this is an attractive picture, it is still somewhat controversial. The LHS sometimes shows a soft component whose temperature and luminosity imply a very small emitting area, not consistent with the large radius expected for a truncated disc (Rykoff et al 2007; Reis et al 2010). While some of this can be explained by continuum modelling, irradiation and assumptions about the inner disc boundary condition (e.g. Gierlinski, Done & Page 2007; Makishima et al 2008), there is still an issue for the lowest mass accretion rate spectra (Reis, Miller & Fabian 2009). However, this can still be consistent with the truncated disc picture if this component is instead produced by clumps torn from the edge of the disc in the truncation process (Chiang et al 2010), which might also explain the variability seen in this component (Uttley et al 2011). The radii derived from the iron line profile are even more controversial,

but issues with instrumental effects and continuum modelling again mean that this is not definitive evidence ruling out a truncated disc for the LHS (c.f. Miller et al 2006; Done & Diaz Trigo 2010; Reis et al 2010; Kolehmainen, Done & Diaz Trigo 2011). Thus we assume a truncated disc geometry in this paper, and quantitatively explore its consequences for the emission spectra of BHB.

In particular, we construct a model of the broadband (radio - X-rays) spectrum of a BHB in the LHS, including a synchrotron jet, multicolour black body disc and Comptonisation in a hot inner flow. This is based on theoretical models of the jet, hot flow, and disc, including evaporation of the disc by thermal conduction from the hot flow as the truncation mechanism (Meyer & Meyer-Hofmeister 1994; Liu et al 1999; Mayer & Pringle 2007). Such models have been previously constructed e.g. by Yuan, Cui & Narayan 2005; Yuan et al 2007; Markoff et al 2005; Pe'er & Markoff 2012). Ours differs in that we set specific model parameters from bright LHS data, and then show how the predicted spectra change as a function of decreasing mass accretion rate.

Our Comptonization model includes the effect of seed photons from both the outer disc and self-generated cyclo-synchrotron photons from the hot electrons in the flow interacting with the tangled magnetic fields. We show that the seed photons from the disc decrease as the disc truncation radius increases, hardening the Compton spectrum until these are overtaken by cyclo-synchrotron from the hot electrons in the flow as the dominant seed photons. These increase in luminosity with decreasing mass accretion rate due to lower self-absorption, so the Compton tail softens again. We show that this can quantitatively as well as qualitatively explain the observed change in behaviour of the hard X-ray spectral slope at lower luminosities (Sobolewska et al 2011).

We show that the alternative model in which the change in spectral slope marks a transition to the X-rays being dominated by the jet does not work in simple synchrotron jet models. The jet is radiatively inefficient, so its X-ray emission drops as quickly as that from the hot flow. The jet luminosity is dominated by the kinetic energy of the outflow, which scales with mass accretion rate, but the radiative luminosity from synchrotron scales with the product of the relativistic electron and magnetic field energy densities. Both of these should scale with mass accretion rate, so the jet emissivity scales as the square of mass accretion rate, making it as radiatively inefficient as ADAF models of a hot flow.

## 2 THE FIDUCIAL MODEL

In the following we use scaled radii  $r = R/R_g$  where  $R_g = GM/c^2$ , and mass accretion rates  $\dot{m} = \dot{M}/\dot{M}_{Edd}$ , where the Eddington limit  $L_{Edd} = \eta \dot{M}_{Edd} c^2$  and  $\eta = 0.057$  for a Schwarzschild black hole. This corresponds to an innermost stable circular orbit  $r_{isco} = 6$ .

Our model consists of an outer Shakura-Sunyaev disc, truncated at some radius  $r_{trunc} \geq r_{isco}$  with an inner hot flow interior to this. Evaporation of the cool disc by thermal conduction from a hot corona is known to produce this geometry at low mass accretion rates (Liu et al 2002; Mayer & Pringle 2007), where it typically gives  $r_{trunc} \propto \dot{m}^{-1/2}$  below some critical mass accretion rate,  $\dot{m}_c$ , at which the hot flow collapses (e.g. Czerny et al 2004). The disc is still substantially truncated at this critical mass accretion rate, so we assume  $r_{trunc} = 20(\dot{m}/\dot{m}_c)^{-1/2}$ . The models assume an ADAF solution for the hot flow, which gives  $\dot{m}_c \sim 0.01$  (Esin, Narayan & Yi 1996; Lui et al 2002), but this is likely only an

analytic approximation to a more complex reality. Instead, we take  $\dot{m}_c \sim 0.1$  to better match with observations.

We assume a standard Novikov-Thorne emissivity for a disc from  $r_{out} = 10^5$  to  $r_{trunc}$ , and assume that all this energy thermalises, giving  $L_{disc}$ . The remaining energy from the Novikov-Thorne emissivity from  $r_{trunc}$  to  $r_{isco}$  is available to power the hot flow,  $L_{hot,power}$ . However, a hot flow is most likely radiatively inefficient so we take  $L_{hot} = (\dot{m}/\dot{m}_c)L_{hot,power}$ .

We assume that the hot flow radiates  $L_{hot}$  via Comptonisation and bremsstrahlung. This requires an optical depth and electron temperature. Observations imply that the optical depth for the brightest low/hard states is of order  $\tau \sim 2$  (e.g. Ibragimov et al 2005; Torii et al 2011). We assume that the optical depth of the hot flow scales linearly with mass accretion rate so that  $\tau = 2\dot{m}/\dot{m}_c$ .

Compton cooling depends on the seed photon luminosity. These seed photons are a mixture of both photons from the disc and cyclo-synchrotron photons generated by the electrons interacting with the magnetic field in the hot flow. We assume that the hot flow is a homogeneous sphere. The obvious radius of this sphere is  $r_{trunc}$ , but the emission should be centrally concentrated, so instead we assume that all the energy is dissipated in a region  $r_h = 20$ . At any radius  $r$  in the disc, we calculate the fraction of photons illuminating the hot flow, so the seed photon luminosity,  $L_{seed,disc}$  is given by this integrated over all the disc from  $r_{out}$  to  $r_{trunc}$ . The density of the flow is then  $n \sim \tau/(\sigma_T r_h R_g)$ .

We assume that the flow is a two-temperature plasma, with ion temperature set by the virial temperature as in an ADAF. The temperature then depends on radius,  $kT_{ion} \approx m_p c^2/r$ . We assume that the flow is homogeneous, so take  $kT_{ion} = m_p c^2/r_h$ . Simulations show that the energy density in the tangled magnetic field saturates to  $\sim 10$  per cent of the gas pressure, so  $U_B = B^2/(8\pi) = 0.1n kT_{ion}$ . The cyclo-synchrotron emission from the hot flow then extends as an approximate steep power law from  $\nu_B = eB/(2\pi m_e c) = 2.6 \times 10^6 B$ . However, the majority of this emission is self-absorbed, so the emission peaks instead at the self-absorption frequency  $\nu_{csa} = \frac{3}{2}\nu_B \theta_e^2 x_m$  where the electron temperature  $\theta_e = kT_e/m_e c^2$  (found iteratively, see below) and  $x_m$  typically has values of a few hundred to a few thousand (see Appendix for full details). The luminosity is then  $L_{seed,cyclo} \propto n \nu_{csa}^2 V$  where  $V = \frac{4}{3}\pi r_h^3 R_g^3$  is the volume of the hot flow.

The total seed photon luminosity  $L_{seed} = L_{seed,disc} + L_{seed,cyclo}$ . We take the seed photon energy as the weighted mean of the inner disc temperature and the self-absorption frequency. The electron temperature can then be derived self-consistently from balancing heating ( $L_{hot}$ ) and cooling (determined by  $L_{seed}$ , but also including bremsstrahlung) rates using the publicly available EQPAIR code. This calculates the electron temperature and resulting emission spectrum from a homogeneous sphere, given inputs of the heating power to the electrons, the optical depth and size of the region, and the power and typical energy of the seed photons for Compton cooling (Coppi 1999). This also gives a spectrum which incorporates both bremsstrahlung and Compton components and does not assume that the Compton emission can be approximated as a power law. This is increasingly important as the flow density drops, as each successive Compton order scattering is separated by a factor  $1/\tau$ , making the spectrum increasingly bumpy as the mass accretion rate decreases.

## 2.1 Spectral Changes with Accretion Rate

Fig 1 shows a sequence of model spectra for  $\dot{m} = \dot{m}_c = 10^{-1}$  to  $\dot{m} = 4 \times 10^{-3}$  (i.e.  $r_t = 20$  to 100). Solid lines show the total emission, long dashed, short dashed and dotted lines show the individual components of cyclo-synchrotron, truncated disc and Comptonisation, respectively.

The proportion of luminosity in the disc compared to the hot flow,  $L_{disc}/L_{hot} \approx (\dot{m}/\dot{m}_c)^{-1}(\frac{r_t}{r_{isco}} - 1)^{-1}$ . Since we also know how  $r_t$  depends on  $\dot{m}$  we can simplify this further to  $\approx 0.3(\dot{m}/\dot{m}_c)^{-1/2} \propto r_t$ . Thus decreasing  $\dot{m}$  by a factor of 25 increases the disc truncation radius by a factor of 5 and increases  $L_{disc}/L_{hot}$  by a factor 5. This is not a large factor, but can be roughly seen by eye in Fig 1 by comparing the ratio between the peak  $\nu f_\nu$  flux of the disc and Comptonised emission for the highest and lowest  $\dot{m}$  spectra.

However, the ratio between  $L_{seed,disc}/L_{hot}$  changes by much more than  $L_{disc}/L_{hot}$  as the fraction of seed photons intercepted by the hot flow drops as  $r_t$  increases. The seed photons from the disc which illuminate the hot flow are integrated over the entire disc, but both the disc luminosity and the fraction which are intercepted by the flow will peak at  $r_t$ . Hence  $L_{seed,disc} \approx L_{disc}(r_h/r_t) \arcsin(r_h/r_t) \approx \frac{\dot{m}}{r_t}(r_h/r_t)^2 \propto r_t^{-5} \propto \dot{m}^{2.5}$ . Thus  $L_{seed,disc}/L_{hot} \propto \dot{m}^{2.5}/\dot{m}^2 \propto \dot{m}^{1/2} \propto r_t^{-1}$ . Thus while  $L_{disc}/L_{hot}$  increases by a factor 5 as  $\dot{m}$  decreases,  $L_{seed,disc}/L_{hot}$  decreases by a factor 5 (see red line in Fig 2a). If this were the only source of seed photons, the spectrum should harden substantially. However, there are also seed photons from the cyclo-synchrotron emission. These have  $L_{seed,cyc} \propto n\nu_{csa}^2 \propto n(B\theta_e^2)^2 \propto \dot{m}^2\theta_e^4$ , so  $L_{seed,cyc}/L_{hot} \propto \theta_e^4$ . This increases as  $\dot{m}$  decreases, as  $\theta_e$  increases as accretion rate drops (see below). The green line on Fig 2a shows the internally generated cyclo-synchrotron emission starts to dominate over seed photons from the disc at  $r_t > 60$  (equivalently  $\dot{m} \leq 10^{-2}$ ). Thus the total  $L_{seed}/L_{hot}$  reaches a minimum at this point, and then starts to increase. This change in dominant seed photons can also be seen in Fig 1 as the Compton spectrum extends to lower energies reflecting the lower seed photon energy of the cyclo-synchrotron photons.

The Comptonisation spectral slope is set by  $L_{seed}/L_{hot}$ , so this also shows a minimum corresponding to the minimum  $L_{seed}/L_{hot}$ . Fig 2b shows the resulting 2-10 keV power law index, and 2-200 keV bolometric luminosity,  $L_{2-200}$ . This corresponds well to the observational data from BHB (and AGN) which show a minimum in  $\Gamma$  between  $10^{-3} \leq \dot{m} \leq 10^{-2}$  (e.g. Sobolewska et al 2011). Thus the model is able to quantitatively describe a key observation of the low/hard state, namely that the X-ray spectrum hardens with decreasing  $\dot{m}$  and then softens again by the change in seed photons from the disc to internally generated cyclo-synchrotron. This softening of the Comptonised emission can be seen by eye in the spectra of Fig 1 by comparing the slope of the tail at highest and lowest luminosity.

Fig 2c shows the resulting electron temperature, set from the balance of heating and cooling. The heating rate is  $\propto \dot{m}^2$ , and cooling is predominantly Compton cooling so is  $\propto 4\theta_e\tau L_{seed}$ . At high  $\dot{m}$ , the seed photons are from the disc so the cooling rate is  $\propto 4\theta_e\tau \frac{\dot{m}}{r_t}(\frac{r_h}{r_t})^2$ . Hence  $\theta \propto \dot{m}^{-3/2}$ , quite close to the observed dependence. Conversely, when seed photons from cyclo-synchrotron cooling dominate, the Compton cooling rate is  $\propto 4\theta_e\tau n\nu_{csa}^2$ , where  $\nu_{csa} \propto B\theta_e^2$  so  $\theta_e \propto \dot{m}^{-0.2}$ . The strong increase in seed photons with increasing temperature leads to increasing cooling with decreasing mass accretion rate, which counteracts much of the decrease in cooling from the decrease in optical depth. Thus

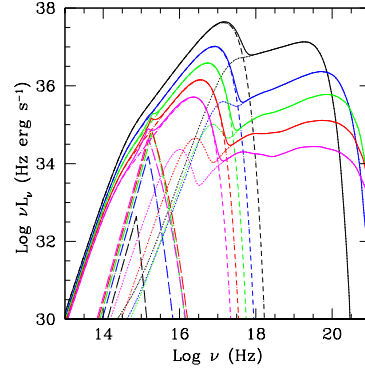


**Figure 1.** Model SEDs, with truncated disc (short dashed line), hot flow cyclo-synchrotron emission (long dashed line) and Comptonisation of both disc and cyclo-synchrotron seed photons (dotted line) for increasing truncation radius:  $20R_g$  (black),  $35R_g$  (blue),  $50R_g$  (green),  $70R_g$  (red) and  $100R_g$  (magenta). The solid line shows the sum of all three components.

the electron temperature increases much more slowly as the mass accretion rate decreases. Again this can be seen in the spectra of Fig 1, where the electron temperature (marked by the high energy rollover of the tail) first increases markedly with decreasing mass accretion rate, then stabilises.

The other obvious change in the Comptonised emission is that it is progressively less well described by a power law as  $\dot{m}$  decreases and  $\tau \ll 1$ . At such low optical depths the individual scattering orders become visible, giving a more complex spectral shape. Data are rarely fit with such low optical depths, as X-ray observations do not show the strong first Compton peak, which would be clearly visible in the X-ray regime if the seed photons were provided by a disc. However, from our model it is clear the dominant source of seed photons at these mass accretion rates is cyclo-synchrotron emission. This brings the first peak out of the X-ray regime, leaving the X-ray spectrum to be dominated by higher order scattering with less extreme curvature.

## 3 JET

The radio jet is an important part of the energy budget of the black hole accretion flow, with kinetic energy which is comparable to the hard X-ray luminosity at  $\dot{m}_c$  (e.g. Cyg X-1: Gallo et al 2005; Russell et al 2007; Malzac et al 2009). We paste a standard conical jet model onto our accretion flow, assuming that some acceleration process operates continuously down the jet, so that a small fraction of the electrons in the jet form a relativistic particle distribution. This has density  $N(\gamma) = K\gamma^{-p}$  for  $1 < \gamma < \gamma_{max}$ , where  $\gamma_{max} = 10^5$  and  $p = 2.4$ . We assume this acceleration occurs from some minimum distance  $Z_0$  (the jet base) out to a distance of  $Z_{max} = 10^6 Z_0$ , where  $Z = zR_g$  is distance along the jet. Distance perpendicular to the jet is  $R_j = \rho R_g = \phi Z$  where  $\phi$  is constant for a conical jet.

### 3.1 Jet at $\dot{m}_c$

We split the jet into segments of volume  $dV = \pi R_j^2 dZ = \pi \phi^2 Z^2 dZ$ . We assume that the relativistic electron density scales inversely with jet volume so  $K(z) = K(z_0)(z/z_0)^{-2}$ . Turbulence probably results in scaling between the relativistic particle and magnetic pressures. Since  $P_B = B^2/(8\pi)$  then this implies

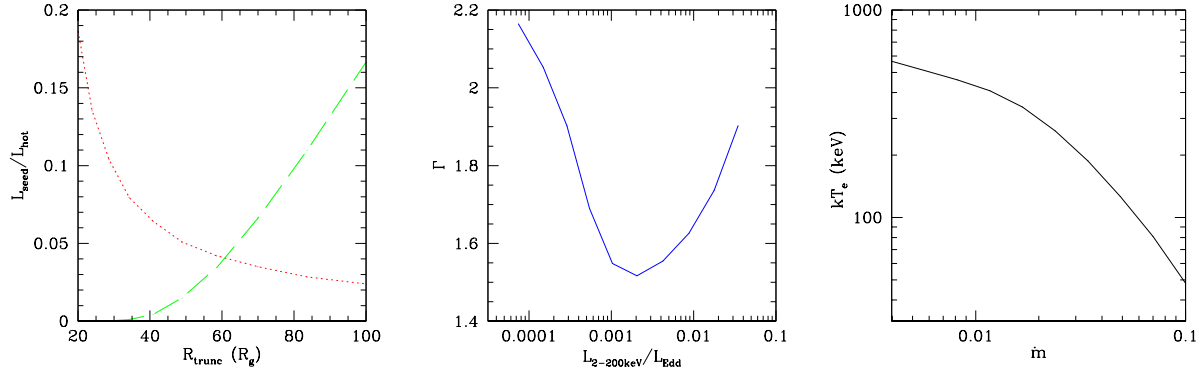


**Figure 2.** a). Seed photon luminosity as a function of truncation radius, for disc seed photons (red solid line) and cyclo-synchrotron seed photons (green dashed line). For  $R_{\text{trunc}} \gtrsim 60R_g$  ( $\dot{m} \sim 0.01$ ) the dominant source of seed photons is cyclo-synchrotron emission from the hot flow itself. b). Photon index as a function of 2-200keV X-ray luminosity, showing softening of the X-ray spectrum at low luminosities as cyclo-synchrotron seed photons begin to dominate. c). Hot flow electron temperature as a function of mass accretion rate, where  $\dot{m} = \dot{M}/\dot{M}_E$ .

$B(z) = B(z_0)(z/z_0)^{-1}$ , and the cyclotron frequency  $\nu_B = 2.6 \times 10^6 B \propto (z/z_0)^{-1}$ .

The  $\delta$  function approximation for the synchrotron luminosity gives  $L(\nu)_{\text{sync}} \propto (P_B/\nu_B)N[(3\nu/4\nu_B)^{1/2}](3\nu/4\nu_B)^{1/2}dV \propto (z/z_0)^{-1}(\nu/\nu_B)^{-(p-1)/2}dZ$ . Since we chose  $p = 2.4$ , this gives a spectrum with energy index  $\alpha = 0.7$  i.e. it rises in  $\nu f_\nu$  with energy output peaking at the highest frequency  $\nu_{\text{max}} = 4/3\gamma_{\text{max}}^2\nu_B$ . Different logarithmic sections of the jet have flux at a fixed frequency which scales as  $\nu_B^{(p-1)/2} \propto (z/z_0)^{-0.7}$ , so this optically thin section of the jet is dominated by emission from the base of the jet.

The power law synchrotron emission becomes optically thick to self-absorption below  $\nu_{\text{ssa}} \propto K^{2/7}B^{5/7}R_j^{2/7} \propto (z/z_0)^{-1}$  (Ghisellini et al 1985) i.e. decreases with larger distance along the jet. The flux at this point,  $L(\nu_{\text{ssa}})_{\text{sync}} \propto (z/z_0)^{-1}(\nu_{\text{ssa}}/\nu_B)^{-(p-1)/2}dZ \propto (z/z_0)^{-1}dZ \propto d \log Z$ . Thus the self absorbed spectra from each part of the jet sum together to produce the characteristic ‘flat spectrum’ (i.e. energy index  $\alpha = 0$ ; Blandford & Koenigl 1979) at low frequencies.

We anchor the jet at  $\dot{m}_c = 0.1$  using observational constraints. The observed break from optically thick to optically thin synchrotron in a bright low/hard state from GX 339-4 is  $\nu_{\text{ssa},0} \sim 10^{13.5}$ , and the 10GHz radio luminosity from the sum of self absorbed jet components is six orders of magnitude below the X-ray emission (Gandhi et al. 2011) i.e.  $\nu L_\nu \sim 10^{31}$  ergs  $s^{-1}$  at 10GHz. We assume that the bulk Lorentz factor  $\Gamma = 1.2$  (e.g. Gallo et al 2005). Beaming alone then collimates the emission into an opening angle of  $1/\Gamma = 0.26$  but we assume that the flow is intrinsically collimated with opening angle  $\phi = 0.1$ . We transform all specific luminosities  $L_\nu$  from jet frame to observer frame by multiplying by  $\delta^3 = (\Gamma - \sqrt{\Gamma^2 - 1} \cos \psi)^{-1}$ , assuming  $\psi = 60^\circ$ , and boost all frequencies by  $\delta$ . We assume the relativistic particles and magnetic energy density scale, so  $U_{\text{rel}} = m_e c^2 \int_1^{\gamma_{\text{max}}} N(\gamma)\gamma d\gamma = f_{\text{rel}} U_B$ . This sets  $B(z_0) \sim 3.5 \times 10^4$  G (i.e.  $K(z_0) = 2.4 \times 10^{12}$  cm $^{-3}$  for  $f_{\text{rel}} = 0.1$ ) and  $z_0 \sim 5300$ .

Fig 3 shows the resulting spectra along the jet for  $\dot{m}_c$ . The drop in  $\nu_{\text{max}}$  and  $\nu_{\text{ssa}}$  with distance along the jet is clearly seen, as is the drop in overall luminosity of the optically thin emission. The total radiated luminosity is  $1.4 \times 10^{37}$  ergs  $s^{-1}$ .

We assume that the jet kinetic energy at  $\dot{m}_c$  is of order that of the bolometric luminosity of the flow i.e.  $L_{KE} \sim 1.4 \times 10^{38}$  ergs  $s^{-1}$ , as determined from observations of Cyg X-1 (Malzac et

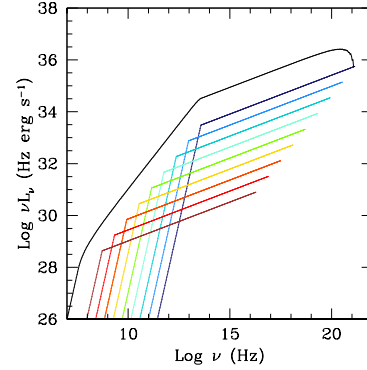


**Figure 3.** Jet spectrum showing emission from each section (blue  $\rightarrow$  red show sections at increasing  $z$ ) and total spectrum in black.

al 2009). Hence the jet radiated luminosity is 10 per cent of the kinetic jet power. However, the fraction of radiative power to kinetic power is not constant down the jet, as the radiation depends on both magnetic and electron energy density so is  $\propto (z/z_0)^{-4}dV$  while the jet kinetic energy is simply  $\propto (z/z_0)^{-2}dV$ .

### 3.2 Jet scaling with mass accretion rate

We then assume that all energy densities scale as  $\dot{m}/\dot{m}_c$  so that  $B(z, \dot{m}) = B(z_0, \dot{m}_c)(z/z_0)^{-1}(\dot{m}/\dot{m}_c)^{1/2}$  and  $K(z, \dot{m}) = K(z_0, \dot{m}_c)(z/z_0)^{-2}(\dot{m}/\dot{m}_c)$ . Fig 4a shows the resulting jet emission together with the disc and hot flow at each  $\dot{m}$ .

Fig 4a shows a sequence of spectra using this coupled accretion flow-jet model. Our model reproduces the  $L_R \propto L_X^{0.7}$  radio-X-ray correlation, as shown in fig 4b. The X-rays come from a radiatively inefficient accretion flow and are therefore proportional to  $\dot{m}^2$ . The radio is from the optically thick jet, where it has a flat spectrum so  $L_R \propto B_0^{1.2}K_0^{0.8} \propto \dot{m}^{1.4}$  for any model where the magnetic energy and particle density scales with  $\dot{m}$ , hence  $L_R \propto L_X^{0.7}$  for a radiatively inefficient X-ray flow (e.g. Heinz & Sunyaev 2003). In fig 5 we superimpose the ‘fundamental plane’ relation of Merloni et al (2003, black line), for a  $10M_\odot$  BH on top of this, showing that our model reproduces this observed relation except at the lowest luminosities, which is due to spectral curvature in our model over the narrow X-ray band used.

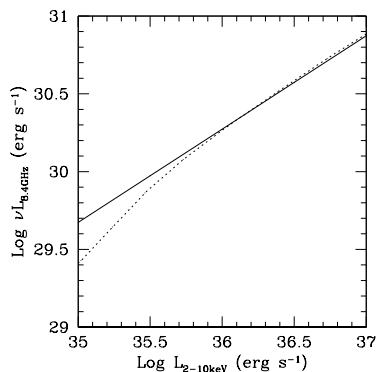


**Figure 5.** Fundamental plane relation (Merloni et al. 2003) scaled to predict 8.4GHz radio flux ( $\log L_R(8.4\text{GHz}) = 0.6\log L_X(2-10\text{keV}) + 0.78\log M + 7.33 + 5/2\log(8.4/5)$ , solid line) together with results from coupled accretion flow-jet model (dotted line), for  $10M_\odot$  black hole.

However, perhaps surprisingly, the jet emission does not ever dominate the hard X-ray emission, but remains an approximately constant factor below the hot flow. This is because the optically thin synchrotron luminosity is  $\propto KUB \propto \dot{m}^2$  so it also follows a radiatively inefficient scaling. This is in contrast to the jet *kinetic* luminosity, which does scale as  $\dot{m}$ . Thus while the *kinetic* luminosity of the jet can easily dominate the radiative energy of the flow, the *radiated* energy of the jet drops as fast as that from the flow. Thus there is no transition in the X-ray spectrum from being dominated by the hot flow to being dominated by the jet.

The alternative explanation is that the X-rays are always dominated by the jet. However our jet model is already very efficient at producing radiation. To make the jet dominate at  $\dot{m}_c$  would require that almost all of the jet kinetic energy was transformed to radiation, which seems unlikely. It would also impact on our assumptions that adiabatic and radiative losses are negligible. Thus we expect that the jet never dominates the hard X-ray flux in these models.

## 4 CONCLUSIONS

We present a model for the broadband spectra (radio - X-rays) of black hole binaries (BHB) in the low/hard state (LHS). The model consists of a truncated black body disc with a radiatively inefficient inner hot flow and synchrotron jet. We scale the truncation radius with accretion rate ( $\dot{m}$ ) such that  $R_{trunc} \propto \dot{m}^{-1/2}$  and examine how the spectrum changes with accretion rate. We then use our model to reproduce the observed radio-X-ray correlation. We summarise our findings:

(i) Cyclo-synchrotron emission takes over from disc emission as the dominant source of seed photons for Comptonisation, as mass accretion rate decreases and truncation radius increases. This occurs at  $R_{trunc} \sim 60R_g$  ( $\dot{m} \sim 10^{-2}$ ) for our fiducial model.

(ii) This change in the dominant source of seed photons produces a minimum in the photon index, with the X-ray spectrum hardening as the disc recedes and then softening again as cyclo-synchrotron seed photons take over. This matches the observed trend in photon index (Sobolewska et al 2011)

(iii) Our combined accretion flow-jet model reproduces the observed  $L_R \propto L_X^{0.7}$  radio-X-ray correlation if the magnetic field and electron density at the jet base scale with accretion rate as  $B_0^2 \propto K_0 \propto \dot{m}$ .

(iv) As a result of this the optically thin jet synchrotron scales as  $L_{X,jet} \propto KUB \propto \dot{m}^2 \propto L_{X,flow}$ . A conical jet obeying the radio-X-ray correlation, combined with a radiatively inefficient accretion flow, does not show a transition from being dominated by X-rays from the accretion flow to being dominated by X-rays from the jet. The X-ray emission from the jet is as radiatively inefficient as the X-rays from the hot flow, although the kinetic energy of the jet scales as  $\dot{m}$ .

## REFERENCES

- Blandford R. D., Königl A., 1979, ApJ, 232, 34  
 Chiang C. Y., Done C., Still M., Godet O., 2010, MNRAS, 403, 1102  
 Coppi P. S., 1999, ASPC, 161, 375  
 Czerny B., Różańska A., Kuraszkiewicz J., 2004, A&A, 428, 39  
 Done C., Gierliński M., Kubota A., 2007, A&ARv, 15, 1  
 Done C., Diaz Trigo M., 2010, MNRAS, 407, 2287  
 Esin A. A., Narayan R., Ostriker E., Yi I., 1996, ApJ, 465, 312  
 Gallo E., Fender R., Kaiser C., Russell D., Morganti R., Oosterloo T., Heinz S., 2005, Natur, 436, 819  
 Gandhi P., et al., 2011, ApJ, 740, L13  
 Ghisellini G., Maraschi L., Treves A., 1985, A&A, 146, 204  
 Gierliński M., Done C., Page K., 2008, MNRAS, 388, 753  
 Heinz S., Sunyaev R. A., 2003, MNRAS, 343, L59  
 Ibragimov A., Poutanen J., Gilfanov M., Zdziarski A. A., Shrader C. R., 2005, MNRAS, 362, 1435  
 Ingram A., Done C., Fragile P. C., 2009, MNRAS, 397, L101  
 Ingram A., Done C., 2011, MNRAS, 415, 2323  
 Ingram A., Done C., 2012, MNRAS, 419, 2369  
 Kolehmainen M., Done C., Díaz Trigo M., 2011, MNRAS, 416, 311  
 Liu B. F., Yuan W., Meyer F., Meyer-Hofmeister E., Xie G. Z., 1999, ApJ, 527, L17  
 Liu B. F., Mineshige S., Meyer F., Meyer-Hofmeister E., Kawaguchi T., 2002, ApJ, 575, 117  
 Makishima K., et al., 2008, PASJ, 60, 585  
 Malzac J., Belmont R., Fabian A. C., 2009, MNRAS, 400, 1512  
 Markoff S., Nowak M. A., Wilms J., 2005, ApJ, 635, 1203  
 Mayer M., Pringle J. E., 2007, MNRAS, 376, 435  
 Merloni A., Heinz S., di Matteo T., 2003, MNRAS, 345, 1057  
 Meyer F., Meyer-Hofmeister E., 1994, A&A, 288, 175  
 Miller J. M., Homan J., Steeghs D., Rupen M., Hunstead R. W., Wijnands R., Charles P. A., Fabian A. C., 2006, ApJ, 653, 525  
 Narayan, R., & Yi, I. 1995, ApJ, 452, 710  
 Pe'er A., Markoff S., 2012, ApJ, 753, 177  
 Reis R. C., Miller J. M., Fabian A. C., 2009, MNRAS, 395, L52  
 Reis R. C., Fabian A. C., Miller J. M., 2010, MNRAS, 402, 836  
 Russell D. M., Fender R. P., Gallo E., Kaiser C. R., 2007, MNRAS, 376, 1341  
 Rykoff E. S., Miller J. M., Steeghs D., Torres M. A. P., 2007, ApJ, 666, 1129  
 Sobolewska M. A., Papadakis I. E., Done C., Malzac J., 2011, MNRAS, 417, 280  
 Torii S., et al., 2011, PASJ, 63, 771  
 Uttley P., Wilkinson T., Cassatella P., Wilms J., Pottschmidt K., Hanke M., Böck M., 2011, MNRAS, 414, L60  
 Yuan F., Cui W., Narayan R., 2005, ApJ, 620, 905  
 Yuan F., Zdziarski A. A., Xue Y., Wu X.-B., 2007, ApJ, 659, 541

## APPENDIX A: ACCRETION FLOW MODEL

The model consists of an outer black body disc (BB), truncated at some radius ( $R_{trunc}$ ), with an inner hot flow of radius  $R_{hot}$ , where  $R_{hot} = 20R_g$ . The hot flow is taken to be radiatively inefficient, such that:

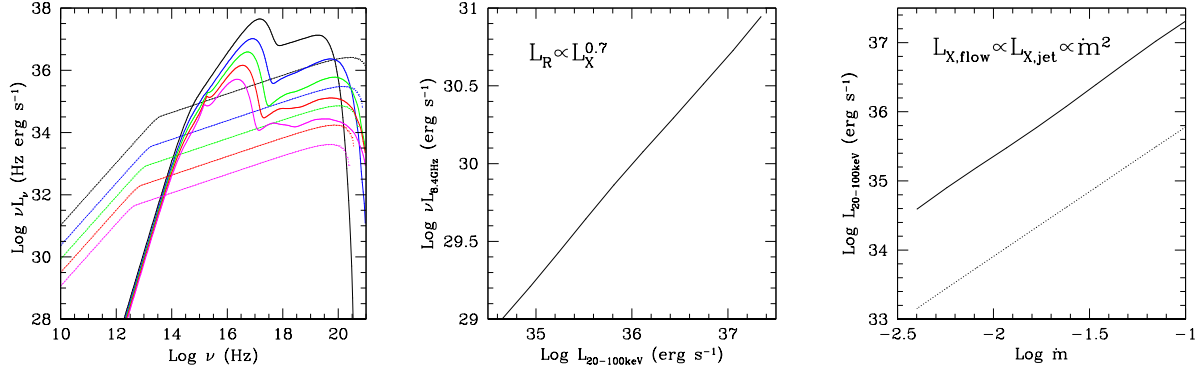


**Figure 4.** a). SEDs, including synchrotron emission from a jet (dotted line) for increasing truncation radius: 20  $R_g$  (black), 35  $R_g$  (blue), 50  $R_g$  (green), 70  $R_g$  (red) and 100  $R_g$  (magenta). b). Radio - X-ray correlation. c). X-ray luminosity as a function of mass accretion rate, where  $\dot{m} = \dot{M}/\dot{M}_E$ , for X-rays from the radiatively inefficient accretion flow (solid line) and X-rays from the jet (dotted line).

$$L_{\text{hot}} = L_{\text{BBdisc}}(R < R_{\text{trunc}}) \left( \frac{\dot{m}}{\dot{m}_c} \right) \quad (\text{A1})$$

Where  $\dot{m} = \dot{M}/\dot{M}_E$ ,  $\dot{m}_c = 0.1$  and  $L_{\text{BBdisc}}(R < R_{\text{trunc}})$  is the luminosity of a BB disc extending from the truncation radius down to the last stable orbit.

We scale the truncation radius with accretion rate, such that:

$$R_{\text{trunc}} = 20 R_g \left( \frac{\dot{m}}{\dot{m}_c} \right)^{-1/2} \quad (\text{A2})$$

The optical depth ( $\tau$ ) of the Comptonising region is fixed at 2 for  $\dot{m} = \dot{m}_c$ , and scales with  $\dot{m}$  as:

$$\tau = 2 \left( \frac{\dot{m}}{\dot{m}_c} \right) \quad (\text{A3})$$

The unabsorbed cyclo-synchrotron emission from the hot flow is calculated following Di Matteo et al. (1997):

$$L_{\text{cyclo}}(\nu) = 5.57 \times 10^{-29} \frac{n\nu I(x)V}{K_2(1/\theta_e)} \quad (\text{A4})$$

Where  $V = 2/3\pi R_{\text{hot}}^3$  is the volume of the Comptonising hot flow,  $n$  is the number density of electrons calculated from the optical depth,  $\theta = kT/m_e c^2$  is the dimensionless electron temperature,  $K_2(1/\theta)$  is the modified Bessel function,  $x = 2\nu/3\nu_B\theta^2$ ,  $\nu_B = eB/2\pi m_e c$  is the Larmor frequency, and the function  $I(x)$  is given by:

$$I(x) = \frac{4.050}{x^{1/6}} \left( 1 + \frac{0.40}{x^{1/4}} + \frac{0.532}{x^{1/2}} \right) \exp(-1.8899x^{1/3}) \quad (\text{A5})$$

The magnetic field ( $B$ ) of the hot flow is calculated from the density by assuming the ions are at the virial temperature and the magnetic field is 10% of the gas pressure, giving:

$$B = \sqrt{0.1 n m_p c^2 \frac{8\pi}{r_{\text{hot}}}} \quad (\text{A6})$$

Where  $r_{\text{hot}} = R_{\text{hot}}/R_g$ . The cyclo-synchrotron self-absorption frequency is given by:

$$\nu_{\text{csa}} = \frac{3}{2} \nu_B \theta^2 x_m \quad (\text{A7})$$

Where  $x_m$  is found by solving for  $x$  when the cyclo-synchrotron and BB emission are set equal:

$$L_{\text{cyclo}}(\nu_{\text{csa}}) = 8\pi^2 m_e \nu_{\text{csa}}^2 \theta_e R_{\text{hot}}^2 \quad (\text{A8})$$

Below the self-absorption frequency the absorbed emission is calculated as:

$$L(\nu < \nu_{\text{csa}}) = \left( \frac{\nu}{\nu_{\text{csa}}} \right)^{5/2} L(\nu_{\text{csa}}) \quad (\text{A9})$$

Thermal Comptonisation is modelled using EQPAIR (Coppi 2002), with seed photons from both the disc and cyclo-synchrotron emission, where the fraction of disc photons from a given radius ( $R$ ) intercepted by the hot flow is given by:

$$\frac{L_{\text{seed,disc}}}{L_{\text{disc}}} = \left( \frac{R_{\text{hot}}}{R} \right) \frac{\arcsin(R_{\text{hot}}/R)}{\pi} \quad (\text{A10})$$

And we calculate the mean seed photon temperature:

$$kT_{\text{seed}} = \frac{k(L_{\text{seed,disc}} T_{\text{disc}} + L_{\text{cyclo}} T_{\text{cyclo}})}{L_{\text{seed,disc}} + L_{\text{cyclo}}} \quad (\text{A11})$$

The electron temperature, a parameter in both the cyclo-synchrotron equations and EQPAIR, is calculated self consistently.

## A1 Jet Model

We construct a conical jet, where opening angle ( $\phi = 0.1$ ) relates jet radius ( $R_j$ ) to distance along the jet ( $z$ ):

$$R_j(z) = \phi z \quad (\text{A12})$$

We assume a fraction of the accreting material ( $f_j$ ) is diverted up the jet. The energy density in relativistic particles at the jet base is set to be some fraction ( $f_{\text{rel}} = 0.1$ ) of the magnetic energy density:

$$m_e c^2 \int_{\gamma_{\text{min}}}^{\gamma_{\text{max}}} \gamma n(\gamma) d\gamma = U_{\text{rel},0} = f_{\text{rel}} U_{B,0} \quad (\text{A13})$$

We conserve magnetic energy density and particle density along the jet such that:

$$B(z) = B_0 \left( \frac{z}{z_0} \right)^{-1} \quad (\text{A14})$$

$$K(z) = K_0 \left( \frac{z}{z_0} \right)^{-2} \quad (\text{A15})$$

And allow  $B_0$  and  $K_0$  to scale with accretion rate as:

$$B_0 = B_0(\dot{m}_c) \left( \frac{\dot{m}}{\dot{m}_c} \right)^{1/2} \quad (\text{A16})$$

$$K_0 = K_0(\dot{m}_c) \left( \frac{\dot{m}}{\dot{m}_c} \right) \quad (\text{A17})$$

Where  $\dot{m}_c = 0.1$ , and  $B_0(\dot{m}_c)$ ,  $K_0(\dot{m}_c)$  and  $z_0$  are fixed by requiring the radio luminosity and the optically thick-optically thin synchrotron break match observations of GX 339-4 (Gandhi et al. 2011).

We assume electrons in the jet are continually accelerated into a power law distribution of the form:

$$n(\gamma) = K\gamma^{-p} \quad (\text{A18})$$

Where  $p = 2.4$ , for electron Lorentz factors ranging from  $\gamma = 1.0 - 1 \times 10^5$ .

We split the jet into conical sections and calculate the synchrotron emission from electrons in each section:

$$L_s(\nu) = \frac{\sigma_{TC}}{8\pi\nu_B} U_B \gamma n(\gamma) V \delta^3 \quad (\text{A19})$$

Where  $V$  is the volume of the conic section,  $\delta = 1/(\Gamma - \cos\psi\sqrt{\Gamma^2 - 1})$  is the boosting factor of the jet,  $\psi$  is the angle of the jet with respect to the observer, and the electron Lorentz factor and synchrotron photon frequency are related by  $\gamma = \sqrt{3\nu/4\nu_B}$ .

The synchrotron self-absorption frequency ( $\nu_{ssa}$ ) in each section is given by (Ghisellini et al. 1985):

$$\nu_{ssa} = \left( 4.62 \times 10^{14} K B^{2.5} \frac{R_j}{0.7} \right)^{2/7} \quad (\text{A20})$$

The frequency of the observed radiation is boosted by a factor  $\nu_{obs} = \nu\delta$ . We neglect synchrotron self-Comptonisation.